Modulation of the organic heterojunction behavior, from electrografting to enhanced sensing properties

Mickaël Mateos, Rita Meunier-Prest, Jean-Moïse Suisse, Marcel Bouvet

Graphical Abstract

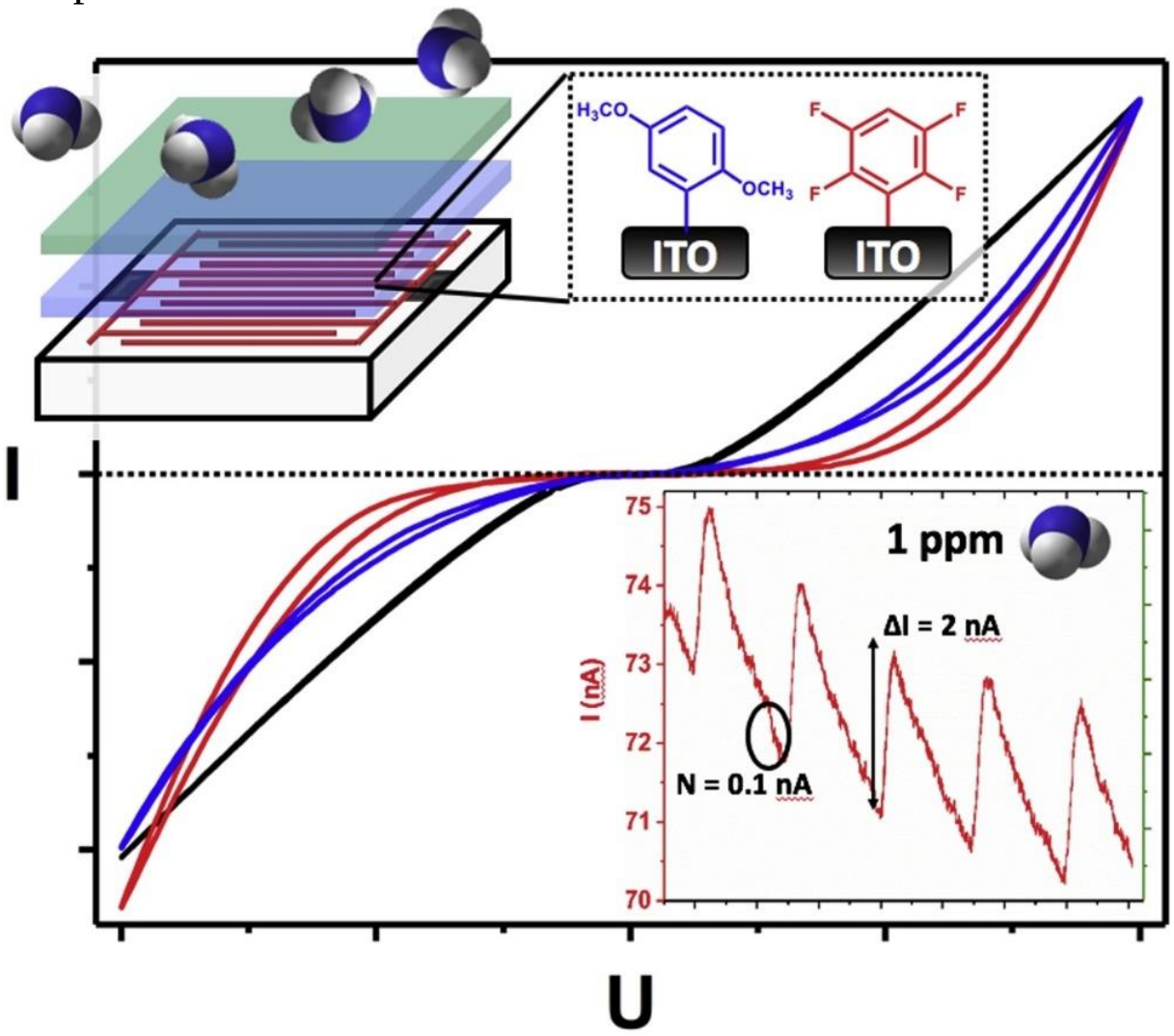

Highlights

- Electrochemical modification of ITO electrodes increases the energy barriers.
- Sensing properties of resistors and heterojunctions are enhanced.
- The sensors operate at RT and in a broad RH range, with a sub-ppm LOD (140 ppb).

Modulation of the Organic Heterojunction Behavior, from Electrografting to Enhanced Sensing Properties

Mickaël Mateos, Rita Meunier-Prest, Jean-Moïse Suisse, Marcel Bouvet**

Institut de Chimie Moléculaire de l'Université de Bourgogne (ICMUB), UMR CNRS 6302, Université Bourgogne Franche-Comté, 9 avenue Alain Savary, 21078 Dijon cedex, France

E-mail: marcel.bouvet@u-bourgogne.fr ; rita.meunier-prest@u-bourgogne.fr

Keywords: molecular materials, organic electronics, diazonium salts, impedance spectroscopy, ammonia sensors

Abstract

The energy barrier of an organic heterojunction built on ITO electrodes and combining a low conductive sublayer ($Cu(F_{16}Pc)$) and a highly conductive semiconductor ($LuPc_2$) is modulated by electrografting of organic layers. Impedance spectroscopy clearly demonstrates the increase of the energy barrier at the ITO – sublayer interface. Additionally, the electrografting is a versatile and promising method for the tuning of heterojunctions. The I(V) characteristics of the heterojunctions are highly modified by the electrografting. The same modifications of electrodes carried out on $LuPc_2$ resistors lead to a modification of their transport properties too. The effect of the grafting of four different aromatic moieties bearing electron-donating and electron-withdrawing substituents was studied. One important feature is that the sensing properties are highly improved compared to the unmodified devices. Thus, the electrografting of dimethoxybenzene doubles the relative response of the heterojunction towards 90 ppm NH_3, as well as the sensitivity in the range 1-9 ppm. This electrografting allows attaining a limit of detection as good as 140 ppb. The modified heterojunctions favorably compete other conductometric transducers for the detection of ammonia, at room temperature and in a broad range of relative humidity.

1. Introduction

In organic electronics, the performances of devices, light emitting diodes, photovoltaic cells and field-effect transistors (OFET) depend not only on the chemical nature, morphology and structure of the materials that compose them, but also on the interfaces. Thus, in OFET the semiconductor-dielectric material interface plays a key role, and in diodes the interface between the p-type and n-type materials as well. Different strategies were developed to modify the electrode-semiconductor interface, like using self-assembled monolayers (SAMs) of thiol derivatives on gold [1-4] or the grafting of organosilicon derivatives or phosphonic acids on oxides, *via* reactions with hydroxyl groups.[3-7] Besides, a particularly powerful method is the electrochemical reduction of diazonium salts [8,9] that leads to the electrografting of organic layers on conducting substrates,[10] including ITO surfaces.[11-14]

Furthermore, we developed new heterojunctions that are not simply a p-n junction between two materials. Combining a low conductive material deposited on interdigitated electrodes with the lutetium bisphthalocyanine, $LuPc_2$, as an intrinsic semiconductor, covering the first layer, we obtained a particular device called MSDI for molecular semiconductor – doped insulator heterojunction,[15-17] and also double lateral heterojunctions.[18]

In the present work, we studied the effect of the electrochemical modification of the ITO – sublayer interface on the response to ammonia of $LuPc_2$ resistors and MSDI heterojunctions. We grafted various benzene derivatives by electrochemical reduction of diazonium salts prepared from a series of aniline derivatives. The quality of the grafting was controlled using a redox probe and by electrochemical quartz crystal microbalance (EQCM). Then, the impact of this functionalization on the behavior of the $LuPc_2$ resistor and the MSDI prepared from the perfluoro-copper phthalocyanine ($CuF_{16}Pc$), as a n-type sublayer, associated with $LuPc_2$, was studied by means of I(V) characteristics and impedance spectroscopy. We related the enhancement of the sensing properties, in particular the limit of detection (LOD), with the

change in electrical behavior of the organic electronic devices caused by electrode surface modification.

2. Experimental Section

Chemicals: 4-Trifluoroethoxyaniline (TFEA), 2,5-dimethoxyaniline (DMA), 2,3,5,6-tetrafluoroaniline (TFA), perchloric acid 70%, sodium nitrite $NaNO_2$ were purchased from Sigma Aldrich and used as received. $K_3Fe(CN)_6$ and $K_4Fe(CN)_6$ were purchased from Arcos Organics and used as received. Absolute ethanol (analaR normapur) was purchased from Carlo Erba. Aniline (Aldrich) was distilled at 120°C under reduced pressure before use. All perchloric acid solutions were prepared by dilution from $HClO_4$ 70 %. Ammonia gas, at 985 and 98 ppm in synthetic air, and synthetic air were used from standard gas cylinders, purchased from Air Liquide, France. Lutetium bisphthalocyanine ($LuPc_2$) and perfluorinated copper phthalocyanine ($CuF_{16}Pc$) (Fig. S1) were synthesized according to previously described methods.[19,20]

Sample preparation: Grafting of the different molecules was performed as follows: a solution of $NaNO_2$ 0.1 M in water and a solution of the aniline derivative 2 mM in $HClO_4$ 1 M were deoxygenated for 15 min with Argon. Then, 40 µL of the first solution was introduced in 1 mL of the second one. The mixture is stirred in the dark, during 5 to 10 min. The deposition was driven by CV (between 25 and 40 cycles) from 0 to -0.65 V at 40 mV s^{-1}. The experiment was stopped after consumption of around 15 mC cm^{-2} and no more evolution of the voltammogram. The modified electrode was rinsed with water, and dried under vacuum at room temperature. $Cu(F_{16}Pc)$, 40 nm in thickness, was deposited on IDEs, by sublimation under secondary vacuum (ca. 10^{-6} mbar), in an UNIVEX 250 thermal evaporator (Oerlikon, Germany). The top layer, $LuPc_2$, 50 nm in thickness, was deposited on the first layer, without breaking the vacuum between the two evaporation steps. $LuPc_2$ resistors were also prepared with the same process

and the same thickness (50 nm). All the evaporations were carried out at a rate of 1 Å s^{-1}, by heating in a temperature range of 400-500 °C.

Electrical and chemosensing measurements: All electrical and sensing measurements were performed at room temperature, using a 6517B Keithley electrometer equipped with an embedded DC voltage supply. The electrometer was controlled through a home-made software relying on a GPIB (IEEE488.2) bus connection for data communication. Current-voltage I(V) curves were registered between -10 and +10 V, while taking care to start and finish at 0 V bias. Impedance data were obtained using a Solartron SI 1260 impedance analyzer. The frequency range was 10 Hz to 10 MHz with a fixed ac oscillation amplitude of 200 or 300 mV and a bias ranging from 0 V to 10 V. A commercial software Zview from Ametek was used for impedance data fitting and parameter extraction. The workbench used for NH_3 exposure, at different relative humidity (rh) values, was described previously.[16] The total flow was in the range 0.5-0.55 nccm depending on ammonia concentration and the volume of the test chamber was 8 cm^3. Gas sensing experiments were carried out in a dynamic way, by alternating 4 min-long rest periods and 1 min-long exposure periods.

3. Results and discussion

3.1. Covalent grafting by reduction of diazonium salts

Because of the strongly fluorinated nature of the Cu(F_{16}Pc) underlayer in the MSDIs, we first opted for depositing a fluorinated layer based on 2,3,5,6-tetrafluoroaniline (TFA) and 4-trifluoroethoxyaniline (TFEA) in order to improve the affinity of the underlayer for the electrodes. For comparison, aniline (ANI) was used as a control and a derivative containing electron-donating groups, 2,5-dimethoxyaniline (DMA) as well. The diazoniums were generated in situ. The voltammograms of the various diazonium salts show a large irreversible reduction peak on the first scan, followed by a rapid collapse of the current over cycles, due to

a progressive passivation of the electrode (Fig. 1). This behavior is typical of a covalent grafting after generation of radicals by the electroreduction of diazonium salts.[10]

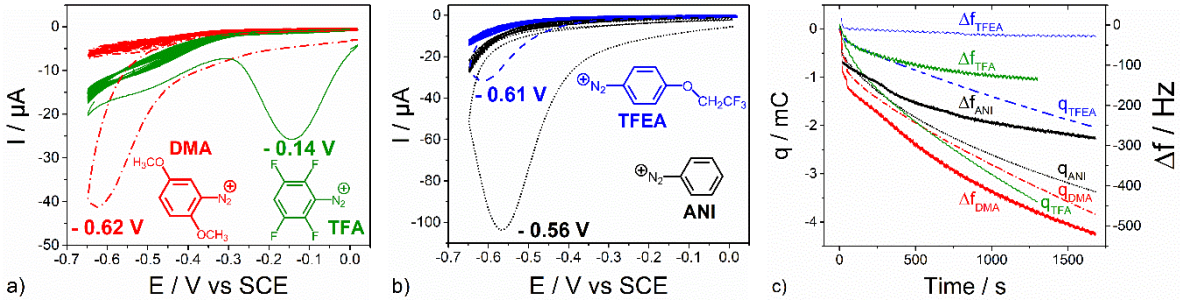

Figure 1. CV on IDE of a) DMA and TFA and b) TFEA and ANI at 2 mM + $NaNO_2$ 4 mM in $HClO_4$ 1 M; v = 40 mV s^{-1} ; c) monitoring of the consumed charge and the variation of frequency in EQCM, in solutions of TFEA, ANI, DMA and TFA.

After reduction of the diazonium function, the use of ANI, DMA, TFA and TFEA leads to the grafting of benzene (Bz), 1,4-dimethoxybenzene (DMBz), 1,2,4,5-tetrafluorobenzene (TFBz) and trifluroethoxybenzene (TFEBz), respectively.

3.2. Electrochemical characterizations

Electrochemical methods are detailed in supplementary materials (S2). Before using these modified IDEs to build devices, the quality of the grafting on ITO substrates was checked using a reversible electrochemical probe, the hexacyanoferrate (III) / (II) couple (Fig. S3). The blocking rate (ratio of the anodic peak current after and before grafting) exceeds 99% for the grafting of DMBz, TFBz and Bz, and 96% for TFEBz, showing a good coverage. In order to guarantee the robustness of the grafting, the stability of the signal was controlled after submitting the modified ITO electrode to ultrasounds for several minutes in water and then in ethanol.

The grafting of the various aniline derivatives was followed by coulometry and EQCM (Fig. 1c). The surface coverage was calculated by coulometry, Γ_q and by EQCM, $\Gamma_{\Delta f}$ (Table 1) (Eq. 1, 2):

$$\Gamma_q = \frac{q}{n*A*F} \qquad (1)$$

$$\Gamma_{\Delta f} = \frac{-\Delta f}{K * M_i} \qquad (2)$$

with q (C) the consumed charge, F (C mol^{-1}) the Faraday constant, A (cm^2) the active area of the electrode, n the number of electrons involved in the reaction, Δf (Hz) the frequency shift measured by EQCM, M_i (g mol^{-1}) the molar mass of the grafted species and K (Hz cm^2 g^{-1}) the calibration factor of the microbalance. The theoretical coverage for a close packed monolayer of benzene is around 5 10^{-10} mol cm^{-2}.[21] This value was used to estimate the number of deposited layers, N_{layers}.

$\Gamma_{\Delta f}$ was low for the fluorinated species, 6.9 and 1.2 10^{-9} mol cm^{-2}, for TFBz and TFEBz, respectively, due to the high steric hindrance and strong hydrophobicity of the fluorine atoms of these two species that inhibit the radical polymerization mechanism responsible for the multilayer formation, whereas it was of the order of 3 10^{-8} mol cm^{-2} for DMBz and Bz, because Bz and DMBz have positions more accessible for polymerization. The grafting tended to a monolayer for TFEBz while the number of layers increased to 60 for DMBz and Bz, evidence that a radical polymerization occurred. The fraction of charge that was actually used to grow film was less than 20% whatever the compound and even lower than 1% for the grafting of TFEBz. Thus, the EQCM allows a more reliable measurement of the surface coverage, which was assumed to be identical on IDE and ITO coated quartz.

3.3. Electrical characterizations of devices

3.3.1. $LuPc_2$ resistor

I(V) characteristics: The I(V) characteristics of modified $LuPc_2$ resistors revealed that the grafting of Bz and TFBz radically changed the behavior of resistors moving from an ohmic regime to a non-linear regime, with a threshold effect at low voltages (Fig. 2a). The threshold voltage, U_{th}, determined by extrapolating to zero current the tangent to the curve at high bias, provides an evaluation of the non-linear character of devices. The TFBz-modified resistor

exhibited a U_{th} of 2.4 V, close to that of an n-MSDI, against 1.4 V with Bz, although the Bz film is thicker than that with TFBz. The fluorine atoms help to raise the energy barrier at the ITO - $LuPc_2$ interface. The grafting of TFBz generated a greater threshold effect despite its lower thickness.

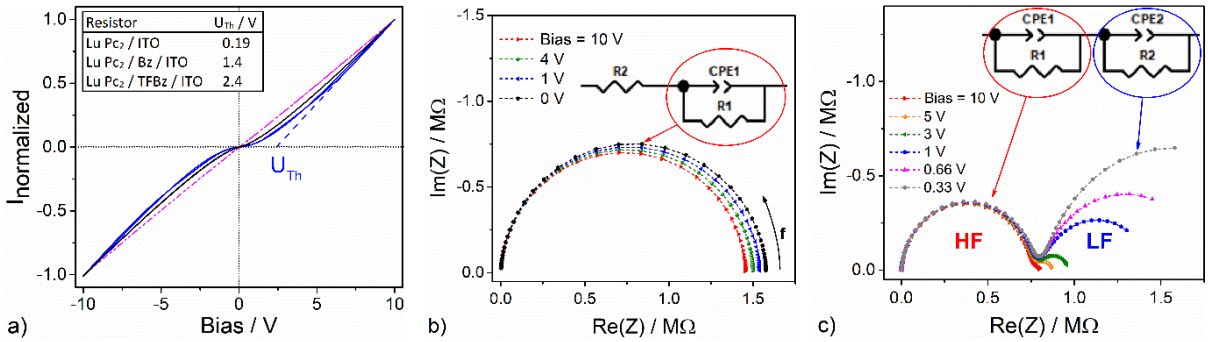

Figure 2. a) Current-voltage characteristics standardized by maximum current at + 10 V of an unmodified $LuPc_2$ resistor on an unmodified (pink) and on TFBz-modified (blue) and Bz-modified (black) IDEs; Nyquist diagram according to the bias of $LuPc_2$ resistors, b) without surface modification, c) with grafting of Bz on the surface of the IDE. Frequency 10 Hz - 10 MHz, U_{AC} = 200 mV.

Whereas $LuPc_2$ makes ohmic contact with ITO, the grafting induced electron and hole injection barriers (Fig. S4) that explain the appearance of a threshold voltage.

Impedance spectroscopy: The Nyquist diagram of the resistor made on bare ITO revealed a single semicircle whose diameter decreased slightly from 1.58 MΩ to 1.45 MΩ when the bias went from 0 to 10 V (Fig. 2b). This Nyquist plot was modeled by an equivalent circuit consisting in a R_1-CPE_1 block that corresponds to the electrical properties of $LuPc_2$ (conductivity and permittivity) in series with a resistance (R_2) that corresponds to the metallic contact of the cell. A CPE (Constant Phase Element) represents an imperfect capacitance,[22] its impedance Z_{CPE} being defined as follow (Eq. 3):

$$Z_{CPE} = \frac{1}{Q(j\omega)^{\alpha}} \qquad (3)$$

with $\omega = 2\pi f$, where f is the frequency, Q the non-ideal capacitance, and α a value between 0 and 1 that reflects the non-ideality of the capacitive element.[23]

In order to compare the devices, the effective capacitance, C_{eff} , was calculated for each R-CPE element (Eq. 4) [22]:

$$C_{eff} = R^{\frac{1}{\alpha}-1} * Q^{\frac{1}{\alpha}} \qquad (4)$$

For the $LuPc_2$ resistor, C_{eff} is 6 pF. The α value, very close to 1 (0.97), indicates an homogeneous behavior of the material. The surface modification changed the aspect of the Nyquist diagram, with the appearance of a second circle at low frequency (LF) (Fig. 2c) whose diameter varies significantly with the bias as encountered in n-MSDI.[24] The modeling of the Nyquist diagram of the n-MSDI modified with Bz was based on an equivalent circuit comprising two R-CPE blocks.

The R_1-CPE_1 block, at high frequency (HF), exhibited stable parameters, with an average resistance R_1 of 760 ± 30 kΩ, a mean coefficient α_1 of 0.95 ± 0.01 and an effective capacitance $C_{eff\ 1}$ of 5.8 ± 0.1 pF close to that of the resistor without surface modification. The R_2-CPE_2 block had a totally different behavior, with a huge decreased of R_2 from 2.3 MΩ to 66 kΩ between 0 and 10 V, α_2 went from 0.83 to 0.65 and $C_{eff\ 2}$ varied from 11 to 3.5 nF between 0 and 10 V, i.e. a thousand times greater than $C_{eff\ 1}$, which indicates that the phenomenon related to the R_2-CPE_2 block takes place on a very thin layer. R_2 became lower than R_1 for a bias between 1 and 2 V, which was closed to the threshold voltage previously determined on the I(V) curve. The resistor modified with TFBz showed the same behavior, with R_2 becoming lower than R_1 for a bias of the order of 3 V. All these observations allowed us to conclude that the R_2-CPE_2 block models the energy barrier at the ITO-$LuPc_2$ interface due to the surface modification.

3.3.2. n-MSDIs

I(V) characteristics: The influence of the surface modification of IDE on the electrical behavior of n-MSDI Cu(F_{16}Pc) (40 nm) - $LuPc_2$ (50 nm) was studied. On the normalized curves, the TFBz grafting involved a broadening of the plateau at low current compared to the non-

modified n-MSDI (Fig. 3). On the contrary, the grafting of TFEBz and DMBz caused only a small increase in the non-linear character of the I(V) curve.

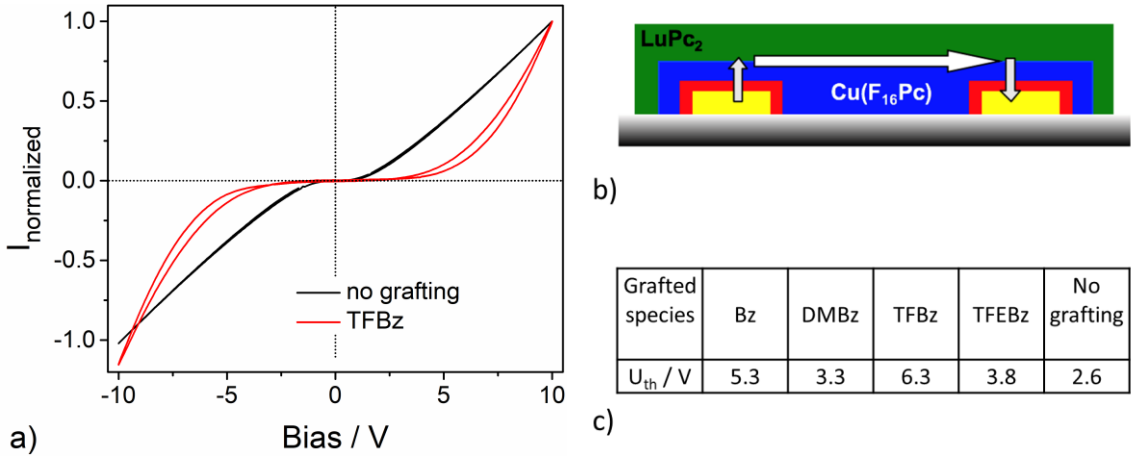

c)

Grafted species	Bz	DMBz	TFBz	TFEBz	No grafting
U_{th} / V	5.3	3.3	6.3	3.8	2.6

Figure 3. a) Current-voltage characteristics normalized by the maximum current at + 10 V of a n-MSDI Cu(F_{16}Pc) – $LuPc_2$ on TFBz - modified IDEs (red) and on unmodified IDEs (black); b) schematic view of the heterojunctions, the arrows indicate the main channel for charge carrriers; and c) threshold voltage of different n-MSDIs, depending on the nature of the performed grafting.

The threshold voltage allowed a better comparison of the impact of the different graftings. The TFBz and Bz graftings resulted in a large increase of U_{th}, at 6.3 and 5.3 V (Fig. 3c), respectively, compared to 2.6 V for the ungrafted MSDI. On the contrary, the grafting of DMBz and TFEBz did not significantly increase the energy barrier (3.3 and 3.8 V, respectively). So, U_{th} increases in the order DMBz < Bz < TFBz. This is clearly related to the chemical nature of the grafted layer, namely the fluorinated benzene leads to the strongest effect, whereas the benzene bearing electron-donating groups (DMBz) leads to the lowest effect. TFEBz has a lower effect than Bz because of the very thin deposited layer The origin of this variation of the interfacial energy barrier is known to result from the modification of the electrode workfunction because of the formation of interface dipoles.[1,7]

Impedance spectroscopy: The n-MSDI Cu(F_{16}Pc) (40 nm) - $LuPc_2$ (50 nm) without surface modification exhibited two semicircles. The first at HF was almost independent of the bias and

the second at LF underwent a decrease of its diameter when the bias increased (Fig. 4a), whereas the LF semicircle became lower than the HF semicircle above 3 V and eventually negligible at 10 V.

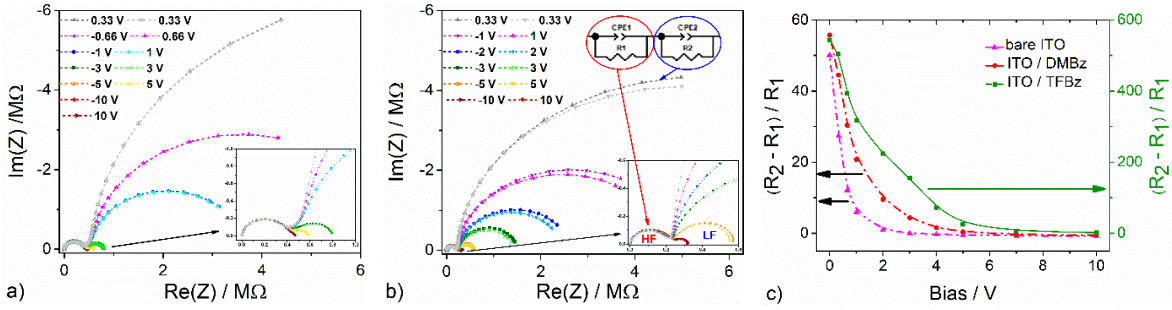

Figure 4. Nyquist diagram at different bias values of n-MSDI Cu(F_{16}Pc) (40 nm) - $LuPc_2$ (50 nm), a) on unmodified IDE; b) with grafting of DMBz, with low impedance zoom and equivalent circuit in inserts; c) comparison of the threshold effect of modified n-MSDIs through the evolution of $(R_2 - R_1) / R_1$ as a function of the bias. The pink (bare ITO) and red (ITO / DMBz) curves are linked with the left Oy axis and the green curve (ITO / TFBz) with the right Oy axis, respectively. Frequency 10 Hz - 10 MHz, U_{AC} = 300 mV.

The surface modification did not modify the overall shape of the diagram (Fig. 4b), but affected the relative size of the two semicircles. In the absence of grafting, the LF semicircle became smaller than the HF semicircle at a bias of 3 V, but this limit voltage shifted towards 5 V (Fig. 4b) with the grafting of DMBz and even exceeded 10 V with TFBz. For the latter, the increase in the diameter of the LF semicircle was extremely high at low bias. The study by impedance spectroscopy confirmed that the surface modification exalts the threshold effect of the devices by increasing the energy barriers.

As for the modified resistors, the device can be modeled by two R-CPE in series (Fig. 4b) as detailed in supplementary materials (Fig. S5).

The evolution $(R_2 - R_1) / R_1$ provided an evaluation of the predominance of interface effects for the different modified n-MSDIs (Fig. 4c). Indeed, R_2 modeled the charge transfer resistance of the interfaces whereas R_1 is related to the conductivity of the different materials. It was clearly shown that the surface modification extended the preponderance of the effect of

interfaces when R_2 is greater than R_1. For the non-grafted device, the ratio vanished between 3 and 4 V, whereas it was canceled between 5 and 7 V for n-MSDI with DMBz and beyond 10 V with TFBz. The impedance spectroscopy behavior of the n-MSDI with grafting of TFEBz and Bz was very near this of the devices modified by DMBz and TFBz, respectively.

3.4. Ammonia detection in a humid environment

3.4.1. $LuPc_2$ resistor

The pristine $LuPc_2$ resistor was a poor ammonia sensor with a very low current variation under ammonia and an important drift of the baseline (Fig. 5a). On the contrary, the resistor with a Bz grafting exhibited an excellent baseline stability and a clear decrease under NH_3, in agreement with the p-type nature of $LuPc_2$ in the air (Fig. 5b).

The sensor measurements were studied at various bias values, with an optimal response at 0.5 V, i.e. below the U_{th} value determined from the I(V) characteristics. Plotting the calibration curves in the range 10 - 90 ppm emphasized the impact of the surface modification of ITO (Fig. S6). The relative response RR of the device is defined as (Eq. 5):

$$RR\ (\%) = \frac{I_f - I_0}{I_0} * 100 \qquad (5)$$

where I_f and I_0 are the current at the end of the exposure phase (1 min) and of the recovery phase (4 min), respectively.

Grafting increased $|RR|$ at 90 ppm NH_3, from 0.9 % for the reference resistor to 8.5 % and 12.6 % for devices modified by TFBz and Bz, respectively. Thus, the surface modification provided a threshold effect that broke the ohmic regime of the $LuPc_2$ resistor and gave it more interesting sensing properties, as soon as the chosen bias was below the threshold voltage.

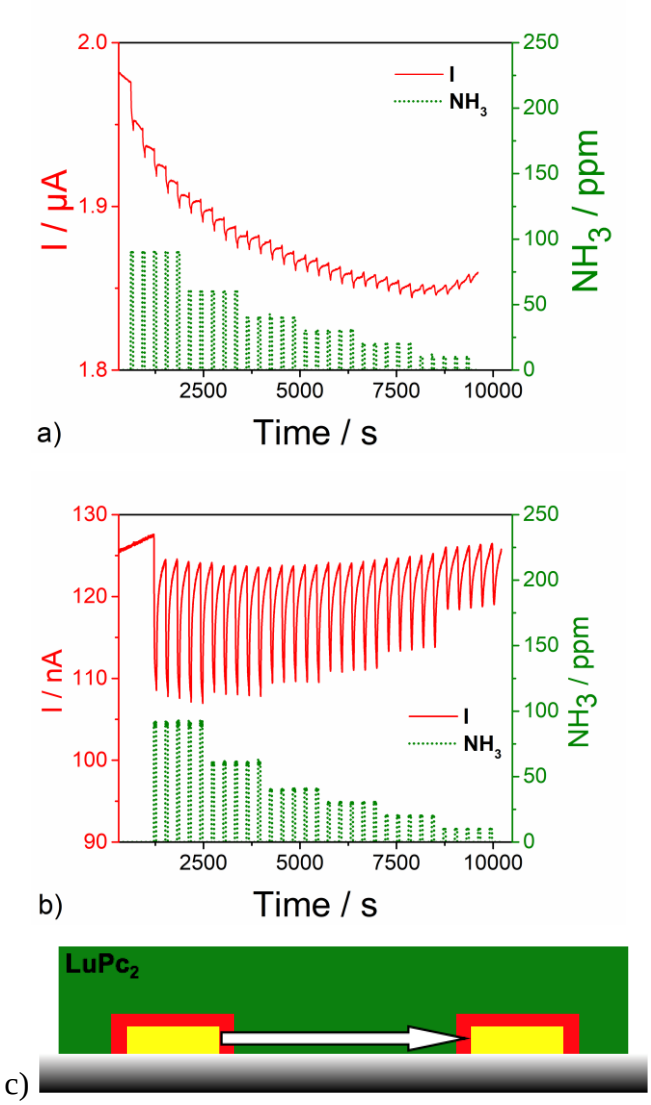

Figure 5. Current response through NH_3 exposure / recovery cycles of 1 min / 4 min, at 50% relative humidity, of a $LuPc_2$ resistor prepared: a) on bare ITO, b) on ITO with grafting of benzene; c) schematic view of the modified resistor. Polarization of 1 V for the bare ITO and 0.5 V for the ITO/Bz curve.

2.4.2. n-MSDI Cu(F_{16}Pc) - $LuPc_2$ on modified ITO

Response to ammonia in a humid environment: For the DMBz-modified MSDI, a significant increase in the current was observed under NH_3, in accordance with the n-type nature of the fluorinated phthalocyanine (Fig. 6). The baseline of the sensor remained generally stable at constant humidity. It decreased only from 61 to 47 nA (bias = 1 V) when the relative humidity (rh) decreased from 50 to 10 %. The shift of the baseline was greater between 70 and 50% rh because the time of preconditioning between these two moisture levels was higher than for the

other transitions. Water and ammonia are electron-donating species that neutralize holes in the $LuPc_2$ layer and in turn increase the density of negative minority carriers in this top layer. Thus, the response was determined by the minority charge carriers, as already reported in the particular case of ambipolar sensing molecular materials.[25] The relative response of the sensor to ammonia was little affected by the moisture content. For a concentration of 90 ppm, the RR value was between 120 and 147 % over the entire humidity range, while it was between 94 and 117% at 60 ppm and finally between 62 and 80% at 30 ppm. Actually, this result is remarkable if we keep in mind that 70% rh corresponds to about 1.68 x 10^4 ppm water at room temperature. The response of the sensor was also determined in the range 1 - 9 ppm at a constant humidity of 50%. The current increased sharply by 22 nA at 9 ppm of ammonia against 2 nA at 1 ppm, with an excellent signal-to-noise ratio (Fig. 6b), which will lead to a sub-ppm detection limit, as hereafter detailed.

The grafting of DMBz induced important changes in the sensor response of n-MSDI. Thus, in all the NH_3 range, RR of the DMBz-modified sensor was about twice this of the unmodified MSDI (Fig. 6c).

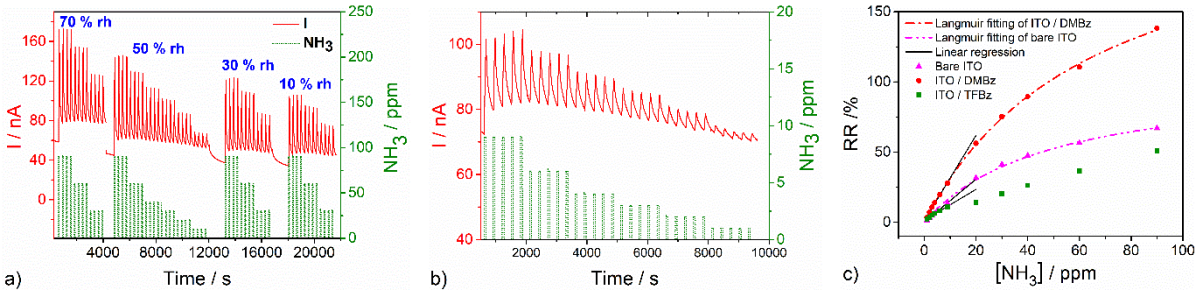

Figure 6. a) Current response of a Cu(F_{16}Pc) - $LuPc_2$ n-MSDI modified with DMBz, upon exposure to ammonia via exposure / recovery cycles of 1 min / 4 min, at different rh values. An additional 1500 s conditioning period between 70 and 50 % rh was not presented; b) response of the same sensor at low concentrations of ammonia (1-9 ppm) and at a constant rh value (50 %); c) relative responses RR of the different n-MSDIs in the range 1 - 90 ppm of ammonia, at 50% rh, with the Langmuir fittings and the sensitivity determination by linear regression in the range 1 - 9 ppm (modeling parameters in Table S1 and S2). All the measurements were performed at 1 V.

On the contrary, TFBz grafting that led to a higher threshold voltage altered the ammonia detection of n-MSDI Cu(F_{16}Pc) - $LuPc_2$, with a very weak I_0 value, namely 30 nA at 50% rh and 20 nA at 10% rh, in spite of a bias of 2 V, against 1 V for the DMBz- modified device. At low ammonia concentration, the sensor response at 1 ppm was hardly noticeable. This indicates that the energy barrier participates to the sensor performances but only up to a limit value.

Calibration curves: The DMBz-modified MSDI exhibited a sensitivity S, defined as the slope the curve RR=f([NH_3]), of 0.98 % ppm^{-1} in the range 40-90 ppm NH_3, but up to 3.0 % ppm^{-1} in the range 1 - 9 ppm, i.e. twice this of the pristine MSDI. The sensor response followed the behavior of a Langmuir adsorption isotherm, characterized by a quasi linear regime at low concentration and a saturation of the response at high concentration (Fig. 6c, Table S2). This model indicates that the maximal sensitivity could attain 3.6%.ppm^{-1} for concentrations lower than 1 ppm. Taking into account I_0 (70 nA) and the noise at 1 ppm (0.1 nA), this device revealed a LOD (Eq. 6) of 140 ppb.

$$LOD = \frac{3N}{S*I_0} \qquad (6)$$

where S is the sensitivity in the 1 - 9 ppm range, I_0 and N are the baseline current and the noise, determined at 1 ppm on the curve I(t).

The n-MSDI without surface modification, reported previously, had never been the subject of studies at low concentrations. Taking into account its sensitivity (1.52% ppm^{-1}, below 10 ppm NH_3), its I_0 (511 nA) and the noise at 1 ppm (0.7 nA), a LOD of 280 ppb was deduced. Contrary to DMBz, the grafting of TFBz degraded the sensing performances of MSDI. Indeed, for the latter, the sensitivity at low concentration dropped to 1.1 %.ppm^{-1} and the noise increased to 0.3 nA leading to a LOD of 2 ppm. The grafting of TFEBz modifies very weakly the sensing properties of the n-MSDI. This device exhibited a sensitivity of 1.35 %.ppm^{-1} in the range 1 - 9 ppm and a RR of 45% to 90 ppm. This behavior was similar to that of the sensor modified with Bz.

It appears that the sensitivity of n-MSDI depends on the energy barriers at the p-n heterojunction between $LuPc_2$ and $Cu(F_{16}Pc)$ and at the electrode – sublayer interface. Indeed, the sensing measurements were carried out with a bias value lower than the total energy barrier, i.e. at a voltage where the current was limited by this energy barrier. The RR of n-MSDIs decreased when the voltage was increased, a too strong bias abolishing the energy barrier effect.

3.4.3. Comparative overview

We summarized the relative response of the present devices, with modified and unmodified electrodes, to a given concentration of ammonia, their average sensitivity and their LOD, by comparing them with the literature (Table 2). The n-MSDI $Cu(F_{16}Pc)$ - $LuPc_2$ with grafted DMBz is the best MSDI developed in the laboratory.[16,26] Its sensitivity was of the same order of magnitude as the polymer-based devices [27-31] but lower than devices made from graphene [32] for which desorption is obtained by heating at ca. 200°C, or from hybrid materials, e.g. those that contain carbon nanotubes and gold nanoparticles (AuNP).[33] The grafted n-MSDI is not the most sensitive but has the great advantage of operating in a humid environment unlike the other reported devices.[34,35] Indeed, humidity, because of its high concentration, is the main interfering gas for most of NH_3 sensors. On the other hand, the excellent sensitivity of the devices based on tungsten oxide and molybdenum was obtained at very high operating temperature (450 °C),[34] while the present organic devices have the advantage of operating at room temperature. Finally, the heterojunctions exhibit very good signal over noise ratios that lead to excellent LOD, comparable to the best LOD reported in the literature,[30,33] and even better for the DMBz modified MSDI.

4. Conclusion

Functionalization of ITO was carried out by reduction of four diazonium salts in aqueous medium. Although the blocking rate of a redox probe remained very good in all cases, the

EQCM measurements revealed that the trifluoroethoxy group in the para position led to a very thin film, near a monolayer, the formation of about ten monolayers for the grafting of TFBz and up to several tens of monolayers for the grafting of Bz and DMBz.

In the case of $LuPc_2$ resistors, the surface modification induced the ITO-$LuPc_2$ interface did not form anymore an ohmic contact and the I(V) characteristics became nonlinear. By impedance spectroscopy, grafting revealed a second semicircle at low frequency associated to interfacial effects. The n-MSDIs that display nonlinear I(V) characteristics saw their threshold voltage increase by the modification of the ITO-Cu($F_{16}Pc$) interface. It highlights that the detection capacity of n-MSDI was due to the energy barrier coming from the p-n heterojunction and from the interface between the electrodes and the sublayer. The interaction between NH_3 molecules and $LuPc_2$ modifies the density of majority charge carriers and therefore indirectly the depletion zone that limits the current through the device. About ammonia detection, the surface modification significantly increased the relative response of $LuPc_2$ resistors that went from 0.9 % at 90 ppm to 12 %, after grafting of benzene. In the case of n-MSDI, the results were more contrasted; with DMBz, the sensitivity of the device was doubled, from 1.5 to 3 $\%.ppm^{-1}$, in the range 1 - 9 ppm, compared to n-MSDI without surface modification, whereas it decreased for the other graftings. These experiments provided for the first time the LODs of n-MSDI, reaching 140 ppb for the most efficient one. It is worth noting that all the studies were achieved at room temperature in a humid environment. This work paves the way for the use of such conductometric sensors not only in the field of air quality monitoring but also in the field of health diagnosis by measurement in human breath. It also highlights the possibility of improving the performance of existing sensors by electrochemical modifications of electrodes, whatever the sensing material used.

Acknowledgements

The authors acknowledge the *Agence Nationale de la Recherche* for funding through the ANR project OUTSMART ANR-2015-CE39-0004-03 and the MENESR for a PhD grant (M. M.). Financial support from the European Union (FEDER) and the *Conseil Régional de Bourgogne* through the FABER and the PARI SMT 08 and CDEA programs is gratefully acknowledged. We also acknowledge the *Conseil Régional de Bourgogne* through the CPER program.

References

[1] H. Kim, Z. Meihui, N. Battaglini, P. Lang, G. Horowitz, Large enhancement of hole injection in pentacene by modification of gold with conjugated self-assembled monolayers, Org. Electron. 14 (2013) 2108–2113. doi:10.1016/j.orgel.2013.04.051.

[2] X. Cheng, Y.-Y. Noh, J. Wang, M. Tello, J. Frisch, R.P. Blum, et al., Controlling electron and hole charge injection in ambipolar organic field-effect transistors by self-assembled monolayers, Adv. Funct. Mater. 19 (2009) 2407–2415. doi:10.1002/adfm.200900315.

[3] A. Ulman, Formation and structure of self-assembled monolayers, Chem. Rev. 96 (1996) 1533–1554.

[4] J.J. Gooding, S. Ciampi, The molecular level modification of surfaces: from self-assembled monolayers to complex molecular assemblies, Chem. Soc. Rev. 40 (2011) 2704–2718. doi:10.1039/c0cs00139b.

[5] P.J. Hotchkiss, S.C. Jones, S.A. Paniagua, A. Sharma, B. Kippelen, N.R. Armstrong, et al., The modification of indium tin oxide with phosphonic acids: mechanism of binding, tuning of surface properties, and potential for use in organic electronic applications, Acc. Chem. Res. 45 (2012) 337–346. doi:10.1021/ar200119g.

[6] I. Lange, S. Reiter, M. Pätzel, A. Zykov, A. Nefedov, J. Hildebrandt, et al., Tuning the work function of polar zinc oxide surfaces using modified phosphonic acid self-assembled monolayers, Adv. Funct. Mater. 24 (2014) 7014–7024. doi:10.1002/adfm.201401493.

[7] M. Aghamohammadi, R. Rödel, U. Zschieschang, C. Ocal, H. Boschker, R.T. Weitz, et al., Threshold-voltage shifts in organic transistors due to self-assembled monolayers at the dielectric: evidence for electronic coupling and dipolar effects, ACS Appl. Mater. Interfaces. 7 (2015) 22775–22785. doi:10.1021/acsami.5b02747.

[8] M. Delamar, R. Hitmi, J. Pinson, J.M. Saveant, Covalent modification of carbon surfaces by grafting of functionalized aryl radicals produced from electrochemical reduction of diazonium salts, J. Am. Chem. Soc. 114 (1992) 5883–5884. doi:10.1021/jacsat.1992.114.

[9] L. Santos, J. Ghilane, J.-C. Lacroix, Formation of mixed organic layers by stepwise electrochemical reduction of diazonium compounds, J. Am. Chem. Soc. 134 (2012) 5476–5479. doi:10.1021/ja300224c.

[10] D. Bélanger, J. Pinson, Electrografting: a powerful method for surface modification, Chem. Soc. Rev. 40 (2011) 3995–4048. doi:10.1039/c0cs00149j.

[11] M. Lo, A.K.D. Diaw, D. Gningue-Sall, J.-J. Aaron, M.A. Oturan, M.M. Chehimi, The role of diazonium interface chemistry in the design of high performance polypyrrole-coated flexible ITO sensing electrodes, Electrochem. Comm. 77 (2017) 14–18. doi:10.1016/j.elecom.2017.02.002.

[12] S. Maldonado, T.J. Smith, R.D. Williams, S. Morin, E. Barton, K.J. Stevenson, Surface modification of indium tin oxide via electrochemical reduction of aryldiazonium cations, Langmuir. 22 (2006) 2884–2891. doi:10.1021/la052696l.

[13] X. Chen, M. Chockalingam, G. Liu, E. Luais, A.L. Gui, J.J. Gooding, A Molecule with Dual functionality 4-aminophenylmethylphosphonic acid: a comparison between layers formed on indium tin oxide by in situ generation of an aryl diazonium salt or by self-assembly of the phosphonic acid, Electroanalysis. 23 (2011) 2633–2642. doi:10.1002/elan.201100337.

[14] L. Santos, J. Ghilane, J.-C. Lacroix, Surface patterning based on nanosphere lithography and electroreduction of in situ generated diazonium cation, Electrochem. Comm. 18 (2012) 20–23. doi:10.1016/j.elecom.2012.02.003.

[15] M. Bouvet, H. Xiong, V. Parra, Molecular semiconductor-doped insulator (MSDI) heterojunctions: Oligothiophene/bisphtalocyanine ($LuPc_2$) and perylene/bisphthalocyanine as new structures for gas sensing, Sens. Actuators: B. Chem. 145 (2010) 501–506. doi:10.1016/j.snb.2009.12.064.

[16] P. Gaudillat, A. Wannebroucq, J.-M. Suisse, M. Bouvet, Bias and humidity effects on the ammonia sensing of perylene derivative/lutetium bisphthalocyanine MSDI heterojunctions, Sens. Actuators: B. Chem. 222 (2016) 910–917. doi:10.1016/j.snb.2015.09.015.

[17] V. Parra, J. Brunet, A. Pauly, M. Bouvet, Molecular semiconductor-doped insulator (MSDI) heterojunctions: an alternative transducer for gas chemosensing, Analyst. 134 (2009) 1776–1778. doi:10.1039/b906786h.

[18] M. Mateos, R. Meunier-Prest, O. Heintz, F. Herbst, J.-M. Suisse, Comprehensive study of poly(2,3,5,6-tetrafluoroaniline): from electrosynthesis to heterojunctions and ammonia sensing, ACS Appl. Mater. Interfaces. 10 (2018) 19974–19986. doi:DOI: 10.1021/acsami.8b03601.

[19] C. Clarisse, M.T. Riou, Synthesis and characterization of some lanthanide phthalocyanines, Inorg. Chim. Acta. 130 (1987) 139–144. doi:10.1016/S0020-1693(00)85943-5.

[20] J.M. Birchall, R.N. Haszeldine, J.O. Morley, Polyfluoroarenes. Part XIV. Synthesis of halogenophthalocyanines, J. Chem. Soc. C: Org. 0 (1970) 2667–2672. doi:10.1039/j39700002667.

[21] T.C. Kuo, R.L. McCreery, G.M. Swain, Electrochemical Modification of Boron-Doped Chemical Vapor Deposited Diamond Surfaces with Covalently Bonded Monolayers, Electrochem. Solid-State Lett. 2 (1999) 288–290. doi:10.1149/1.1390813.

[22] C.H. Hsu, F. Mansfeld, Technical note: concerning the conversion of the constant phase element parameter Y0 into a capacitance, Corrosion. 57 (2001) 747–748. doi:10.5006/1.3280607.

[23] C.-H. Kim, H. Hlaing, S. Yang, Y. Bonnassieux, G. Horowitz, I. Kymissis, Impedance spectroscopy on copper phthalocyanine diodes with surface-induced molecular orientation, Org. Electron. 15 (2014) 1724–1730. doi:10.1016/j.orgel.2014.04.039.

[24] M. Bouvet, P. Gaudillat, A. Kumar, T. Sauerwald, M. Schüler, A. Schütze, et al., Revisiting the electronic properties of Molecular Semiconductor – Doped Insulator (MSDI) heterojunctions through impedance and chemosensing studies, Org. Electron. 26 (2015) 345–354. doi:10.1016/j.orgel.2015.07.052.

[25] Y. Chen, X. Kong, G. Lu, D. Qi, Y. Wu, X. Li, et al., The lower rather than higher density charge carrier determines the NH_3-sensing nature and sensitivity of ambipolar organic semiconductors, Mater. Chem. Front. 2 (2018) 1009–1016. doi:10.1039/C7QM00607A.

[26] A. Wannebroucq, G. Gruntz, J.-M. Suisse, Y. Nicolas, R. Meunier-Prest, M. Mateos, et al., New n-type molecular semiconductor–doped insulator (MSDI) heterojunctions combining a triphenodioxazine (TPDO) and the lutetium bisphthalocyanine ($LuPc_2$) for

ammonia sensing, Sens. Actuators: B. Chem. 255 (2018) 1694–1700. doi:10.1016/j.snb.2017.08.184.
[27] P. Gaudillat, F. Jurin, B. Lakard, C. Buron, J.-M. Suisse, M. Bouvet, From the solution processing of hydrophilic molecules to polymer-phthalocyanine hybrid materials for ammonia sensing in high humidity atmospheres, Sensors. 14 (2014) 13476–13495. doi:10.3390/s140813476.
[28] T. Patois, J.-B. Sanchez, F. Berger, J.-Y. Rauch, P. Fievet, B. Lakard, Ammonia gas sensors based on polypyrrole films: Influence of electrodeposition parameters, Sens. Actuators: B. Chem. 171-172 (2012) 431–439. doi:10.1016/j.snb.2012.05.005.
[29] N. Van Hieu, N.Q. Dung, P.D. Tam, T. Trung, N.D. Chien, Thin film polypyrrole/SWCNTs nanocomposites-based NH_3 sensor operated at room temperature, Sens. Actuators: B. Chem. 140 (2009) 500–507. doi:10.1016/j.snb.2009.04.061.
[30] J. Jian, X. Guo, L. Lin, Q. Cai, J. Cheng, J. Li, Gas-sensing characteristics of dielectrophoretically assembled composite film of oxygen plasma-treated SWCNTs and PEDOT/PSS polymer, Sens. Actuators: B. Chem. 178 (2013) 279–288. doi:10.1016/j.snb.2012.12.085.
[31] M. Mateos, M.-D. Tchangaï, R. Meunier-Prest, O. Heintz, F. Herbst, J.-M. Suisse, et al., Low conductive electrodeposited poly(2,5-dimethoxyaniline) as a key material in a double lateral heterojunction, for sub-ppm ammonia sensing in humid atmosphere, ACS Sens. 4 (2019) 740–747. doi:10.1021/acssensors.9b00109.
[32] F. Yavari, E. Castillo, H. Gullapalli, P.M. Ajayan, N. Koratkar, High sensitivity detection of NO_2 and NH_3 in air using chemical vapor deposition grown graphene, Appl. Phys. Lett. 100 (2012) 203120. doi:10.1063/1.4720074.
[33] Q. Chang, K. Zhao, X. Chen, M. Li, J. Liu, Preparation of gold/polyaniline/multiwall carbon nanotube nanocomposites and application in ammonia gas detection, J. Mater. Sci. 43 (2008) 5861–5866. doi:10.1007/s10853-008-2827-3.
[34] C.N. Xu, N. Miura, Y. Ishida, K. Matsuda, N. Yamazoe, Selective detection of NH_3 over NO in combustion exhausts by using Au and MoO_3 doubly promoted WO_3 element, Sens. Actuators: B. Chem. 65 (2000) 163–165. doi:10.1016/S0925-4005(99)00413-X.
[35] L. Wang, H. Huang, S. Xiao, D. Cai, Y. Liu, B. Liu, et al., Enhanced sensitivity and stability of room-temperature NH_3 sensors using core-shell CeO_2 nanoparticles@cross-linked PANI with p-n heterojunctions, ACS Appl. Mater. Interfaces. 6 (2014) 14131–14140. doi:10.1021/am503286h.

Table 1. Determination of the surface coverages of the different graftings carried out on quartz covered with ITO, calculated from coulometric and EQCM results.

	DMBz	**Bz**	**TFBz**	**TFEBz**
q/A [mC cm^{-2}]	10.4	19.6	18.3	10.4
-Δf [Hz]	520	280	133	28.3
Γ_q [nmol cm^{-2}]	200	175	186	106
$\Gamma_{\Delta f}$ [nmol cm^{-2}]	25	28	6.9	1.2
N_{layers}	60	56	14	2

Table 2. Summary of the sensing properties (RR, S, LOD) of the present devices compared to the literature.

Devices	RR [%]	$[NH_3]$ [ppm]	S [% ppm^{-1}]	LOD [ppb]	$[NH_3]$ [ppm]	T [°C]	rh [%]	Ref.
$F_{16}CuPc$ – $LuPc_2$ MSDI on bare ITO	67	90	1.5	280	1 - 9	25	50	This work
$F_{16}CuPc$ – $LuPc_2$ MSDI on DMBz / ITO	138	90	3	140	1 - 9	25	50	This work
$F_{16}CuPc$ – $LuPc_2$ MSDI on TFBz / ITO	50	90	1.1	2000	1 - 9	25	50	This work
$F_{16}CuPc$ – $LuPc_2$ MSDI on TFEBz / ITO	45	90	1.3		1 - 9	25	50	This work
PTCDI – $LuPc_2$ MSDI	34	90	0.6		10 - 30	25	50	[16]
TPDO – Lu Pc_2 MSDI	26	90	0.2		30 - 90	25	50	[26]
PTFA – $LuPc_2$ heterojunction	14	90	1.05	450	1 - 6	25	50	[18]
PDMA – $LuPc_2$ heterojunction	14	90	2.23	314	1 - 6	25	50	[31]
PANI-CuTsPc resistor	78	30	1.9		10 - 30	25	50	[27]
PPy resistor	16	40	0.2	1000	40-75	25		[28]
PPy - SWCNT resistor	26	10	0.5		10 - 140			[29]
PEDOT/PSS-SWCNT resistor	33	300	0.21	200	2 - 100			[30]
AuNP-PANI-MWCNT resistor	64	25	6	200	1 - 10			[33]
CVD synthesized graphene resistor	40	40	6 – 0.09*	≈ 500	0.5 – 1000*	25**		[32]
MoO_3-WO_3 resistor	1000	5	200		5			[34]
CeO_2 – PANI resistor	550	50	11		2 - 50			[35]

* non-linear but measured down to 0.5 ppm; ** measured at 25°C but desorption was achieved by heating under vacuum at ca. 200°C